A New Interrogation System for FBG Sensors based on Midband Filter with Correction

Sami Ghedira

Laboratory of Microelectrics and Instrumentation, Faculty of Sciences of Monastir, University of Monastir, Tunisia
sami.ghedira@fsm.rnu.tn (corresponding author)

Said Saad

Electronics team, Laboratory of Quantum and Statistical Physics, Faculty of Sciences of Monastir, University of Monastir, Tunisia
said.saad@fst.rnu.tn

ABSTRACT

In this paper, a midband interrogation system for Fiber Bragg Grating (FBG) sensors is presented and its numerical demonstration is reported. The midband interrogation system is based on a finite reflection filter with automatic correction. The filter is used to interrogate the FBG sensors. The strain FBG sensors were used to demonstrate the effectiveness of the proposed systems. The results demonstrate that the proposed system of interrogation has a great resolution (±1 pm) with good stability.

Keywords-interrogation system; midband; correction; filter; fiber Bragg grating; sensors; strain

I. INTRODUCTION

The FBG technology is proved to be effective in temperature and strain sensors [1] for several fields, such as civil engineering [2-4], health [5], aeronautics, and artificial intelligence in robotics [6]. The FBG technology has many advantages like fast response, high sensitivity and electromagnetic interference opposition [7]. Technically, the center wavelength of the inscribed grating in the fiber changes due to the mechanical effect exerted by external forces such as pressure and temperature [8]. Hence, a good calibration and measurement of the wavelength shift can get the external force [9]. On the other side, to reconstruct the sensing signal, an interrogation system is needed. Actually, there are many interrogation system techniques like the edge filter [10], the low loss jammed-array wideband sawtooth filter [11], tunable lasers [12], and magneto-optic wavemeter [13]. However, many of these techniques are expensive and cannot avoid wavelength fluctuations [13]. Hence, to avoid measurement errors and minimize the cost of the system of the interrogation, we present a new interrogation system based on midband filter integrated in STM 32 card.

II. MIDBAND FILTER

The ordinary interrogation system for FBG sensors is based on the edge filter. This technic has many advantages like simple arrangement, speed detection, and active measurement [14]. Nevertheless, this technic has also several disadvantages like difficult adjustment between the active range and the detection measurement which causes measurement errors. In addition, the linear edge filter is a hard technique [15]. On the other hand, the interrogation system that is based on edge filter needs much speed for the data acquisition system [16-17]. For instance, to create an interrogator FBG of 200 kHz with wavelength that surveying the range about 40 nm and a wavelength resolution of 1 pm, a speed data acquisition system with sampling of 8 GHz is required to rebuild the sensing signal [11]. This equipment is costly. For our interrogation system, we need simply a speed data acquisition system of 0.4 GHz in order to realize the rebuild of the sensing signal. These values reduce in a huge way the cost of the system of interrogation. The proposed filter serves to eliminate the problems mentioned above and make a challenge with the arrayed waveguide grating [18] and the Fabry Perot cavity [19]. In addition, the edge filter for the interrogation system must be accordable and provide for each channel of FBG sensors an individually filter with a midband bandwidth. The frequency response draws of the proposed midband filter is presented in Figure 1. Moreover, we have used as basic circuit for our filter which is mentioned in Figure 2. In addition, the basic transfer function for our filter is:

$$H(p) = \frac{V_o(p)}{V_i(p)} = \frac{\frac{R}{L}p}{p^2 + \frac{R}{L}p + \frac{1}{LC}} \qquad (1)$$

The numeric transfer function for the mentioned filter is:

$$H(z) = \frac{2R(1-z^{-1})}{\frac{4L(1-z^{-1})^2}{T_e(1+z^{-1})} + 2R(1-z^{-1}) + \frac{T_e}{C}(1+z^{-1})} \qquad (2)$$

with T_e is the sampling period. For our filter of 1.5 µm central frequency and 1 nm bandwidth, the simulation gives the curve in Figure 3.
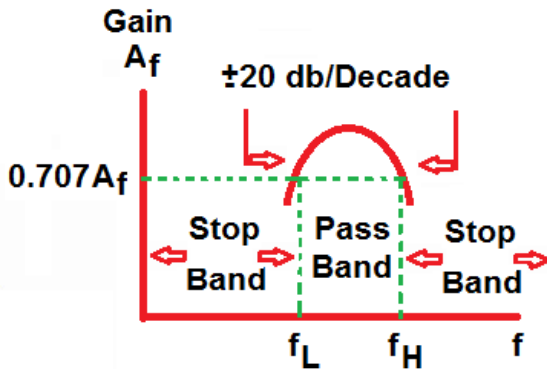

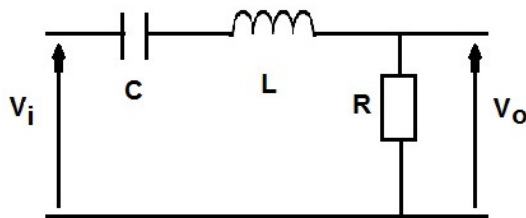Fig. 1.   Frequency response draws of the midband edge filter.

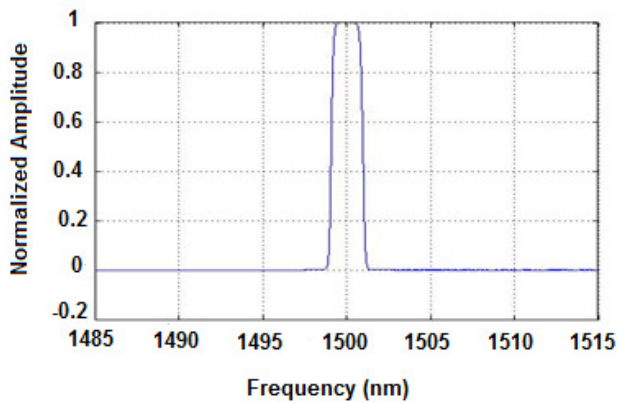Fig. 2.   Basic circuit of the proposed midband edge filter.

Fig. 3.   Frequency response of the proposed filter with 1.5 µm central frequency.

There are two types of bandpass filters: narrow bandpass and wide bandpass filters. The filter type depends on the quality factor Q. Thus Q, is a measure of selectivity: the higher the value of Q the more selective is the filter or the narrower is the bandwidth. However, our model is characterized by a bandwidth of midband type, i.e. the bandwidth is between the narrow and wide bandpass types. We chose to use this type in order to have the measurements of the strains of the FBG sensors done with more reliability and the central bandwidth can be accessible in order to find measurements with more selectivity [20] in the two edges of our filter.

III.   THE INTERROGATION PRINCIPLE

As we know, for different reasons, the output beam from the source may not be collimated, so making a wideband filter is difficult [21]. For this reason, we propose a midband filter for the given bandwidth. In addition, our filer is programmed with an STM 32 card. In the other hand, we can use other edge filters with linear characteristics in order to demodulate the proposed midband filer. In addition, the proposed filter is introduced in the correction system. Therefore, for the proposed system, every wavelength output is monitored during the scan with correction. The equation of our corrector is similar with that of an integrating corrector:

$$C(p) = \frac{1}{T_i \cdot p} \tag{3}$$

The numeric transfer function for the mentioned integrating filter is:

$$C(z) = \frac{T_e(1+z^1)}{2T_i(1-z^{-1})} \tag{4}$$

where T_i is the time constant for integration and T_e is the sampling period. Figure 4 illustrates the equipment of the proposed interrogation system. The high reflectivity of FBG causes a light that is reflected from its end to reenter in the STM 32 card through the circulator and photodiode with optical filter to guarantee a reflected spectrum is in the C band and according to the Bragg wavelength which minimizes the phenomenon of absorption loss [22]. The module in the STM 32 is our midband edge filer with correction. It is designed to be a spatial filter, accordable with the reflected signal of the FBG and gives a high spectral resolution.
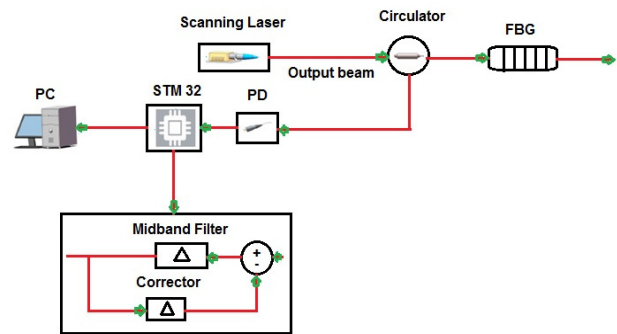

Fig. 4.   Equipment of the proposed interrogation system.

IV.   RESULTS AND DISCUSSION

The benefits of the use of the corrector are the precision improvement and the cancellation of the static error with asymptotic rejection of constant disturbances in the two edges of the proposed filter. The software used in the proposed system inlcuded MATLAB, Optisystem, and STM32Cube. The following parameters of the FBG sensor were considered: Λ = 0.529 µm (grating period), $neff$ =1.456 (the effective refractive index of the fiber), length of 6 mm, and average modulation of the refractive index equivalent to 2.5×10^{-4}. So, the obtained central wavelength of the reflected spectral signal is: λ_B = 1.5425 µm, in correspondence with this expression:

$$\lambda_B = 2. \, n_{eff}. \, \Lambda \qquad (5)$$

Figure 5 gives the shape of reflectivity. This reflectivity is the same shape with that presented in previous research works [23]. The light that reflected from the FBG sensor is easier to enter in the circulator, and then it is transformed in electric signal through the photodiode (PD) according to the Bragg wavelength. The obtained signal will be enter in the STM 32 card where it will be investigated. Our interrogation system of FBG sensors consists of a midband filter and an integrated corrector with a feedback signal as shown in Figure 4. In addition, the traditional filter is restricted by the bandwidth. The proposed midband filter tackles this problem where we can realize a bandwidth of 1 nm to 2 nm and with a duty cycle more than 50%. Moreover, the reflectivity creates the characteristics of the filter and the corrector relatively in two parameters: spectral resolution and the distribution of the output optical intensity. Analogous to the distribution electric intensity, the distribution optical intensity of laser signal of the interrogation system is illustrates in Figures 6 and 7.
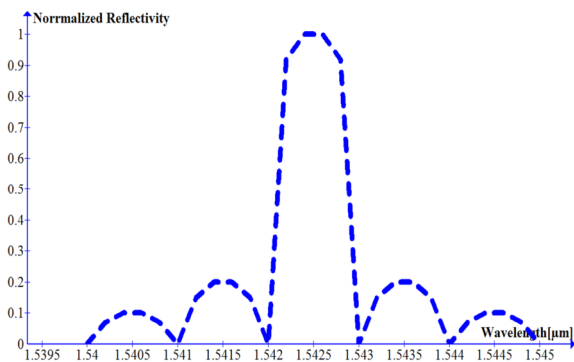

Fig. 5.   Reflectivity shape of the FBG sensor.

In the range of band C (1530 to 1570 mm), the spectrum response of the proposed interrogation system is shown in Figure 6. Figure 7 shows in detail the spectrum response in the range of 1540 nm to 1550 nm with the elimination of the side bands for each spectra in the real case according to improve the numerical calculation. The obtained results illustrate that the periodical spectrum is in the order of 1 nm with a duty cycle of about 50%. These results are suitable with those of other edge filters.

As mentioned above, we have a spectrum with high periodic of resolution in the form of a series of linearly edges. The interrogation system builds on an integration of midband filter and an integrated corrector with a feedback signal in STM 32 card. This equipment is defined with a low price. The optical track in the interrogation system comprises an electrical signal formed through the PD according to the Bragg wavelength that enters the feedback equipment. The spectrum of the interrogation system is similar to those of the reflected signal of the FBG but with a delay as that presented in Figures 6 and 7. The correction of the delay or advance type is realized with the corrector block through the feedback of the electric signal to form a midband edge filter. From the Figures, we can mention that the resolution of the spectrum of the interrogation system is high, up to 50%. This value is suitable to create edge

filter, since the linear edges in the curves of the spectrum filter are slipperier. In order to demonstrate the effectiveness of the proposed interrogation system, we installed our FBG sensors above a rubber pipe (Figure 8). Figure 9 represents the spectrum of the reflected light of our FBG, the center wavelengths of the FBG is 1542.5 nm, with 0 strain. When the iron pipe undergoes external pressure, we have a shift in the center wavelength of FBG sensor (Figure 10), according to the following expression [24]:

$$\Delta\lambda_B = \lambda_B(1 - \rho)\varepsilon \qquad (6)$$

where ρ is the coefficient of the fibre effective photo-elastic and ε is the applied strain.
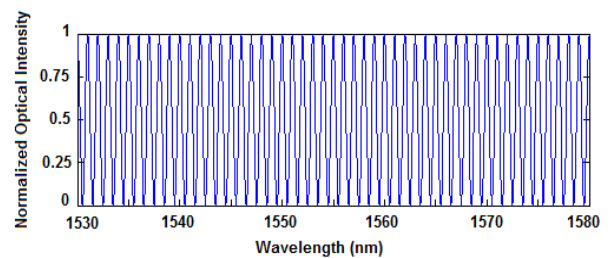

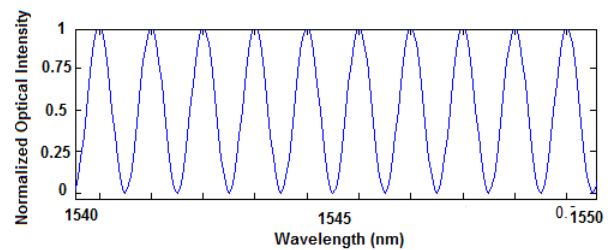Fig. 6.   Spectrum response of the interrogation system.

Fig. 7.   Spectrum response of the interrogation system for the range [1540 nm, 1550 nm] with filter bandwidth of 1 nm and duty cycle filter of 50%.
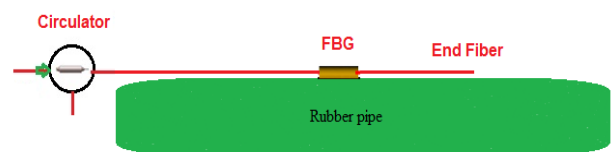

Fig. 8.   Installation of the FBG sensor above a rubber pipe.
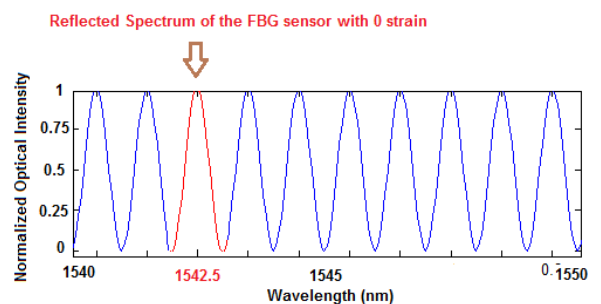

Fig. 9.   The reflect spectrum of the FBG sensor with 0 strain.

Moreover, when the reflected spectrum of the FBG not is identical on the spectrum response of the interrogation system (Figure 11(a)), the shape of the spectrum response of the interrogation system moves to be identical with the reflected spectrum of the FBG sensor according to the correction block in the interrogation system (Figure 11(b)).
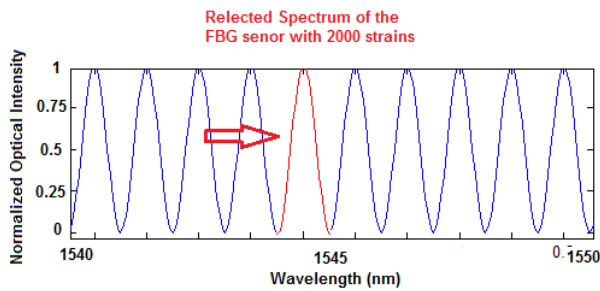

Fig. 10.   The reflect spectrum of the FBG sensor with 2000 strain.

We fixed the two FBGs with the same center wavelength above the rubber pipe with 1m distance between them (Figure 12). Then, an external pressure of 4000 strains above the FBG2 sensor was applied (Figure 13).
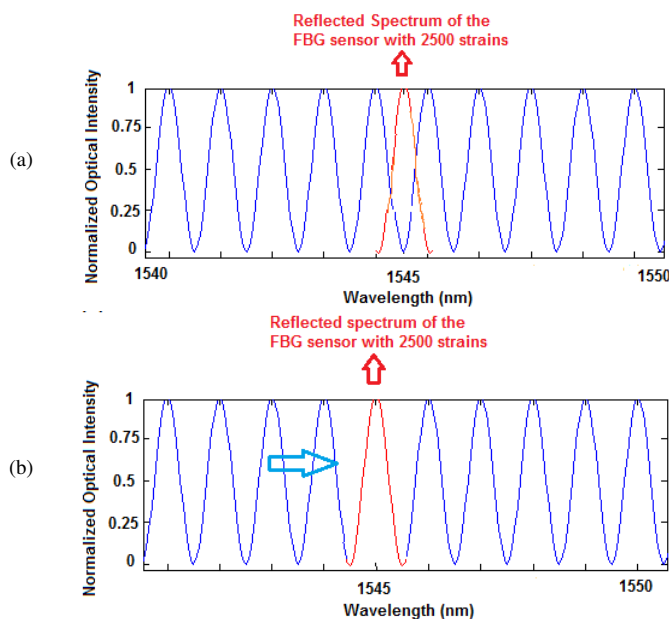

Fig. 11.   (a) The reflected spectrum of the FBG sensor with 2500 strains, (b) the spectrum response of the interrogation system moves to be identical with the reflected spectrum of the FBG sensor according to the correction block in the interrogation system.
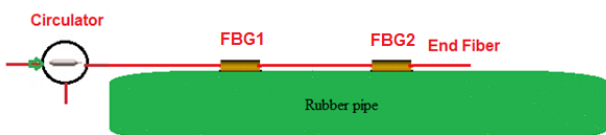

Fig. 12.   Two FBG sensors, FBG1 and FBG2, with the same center wavelength above the rubber pipe with 1 m distance between them.
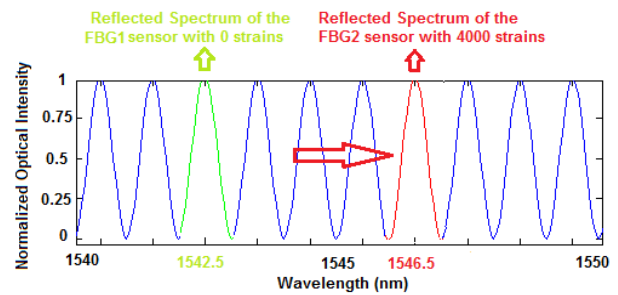

Fig. 13.   The reflected spectrum of the FBG1 and FBG2 sensors with 4000 strains above the FBG2 sensor.
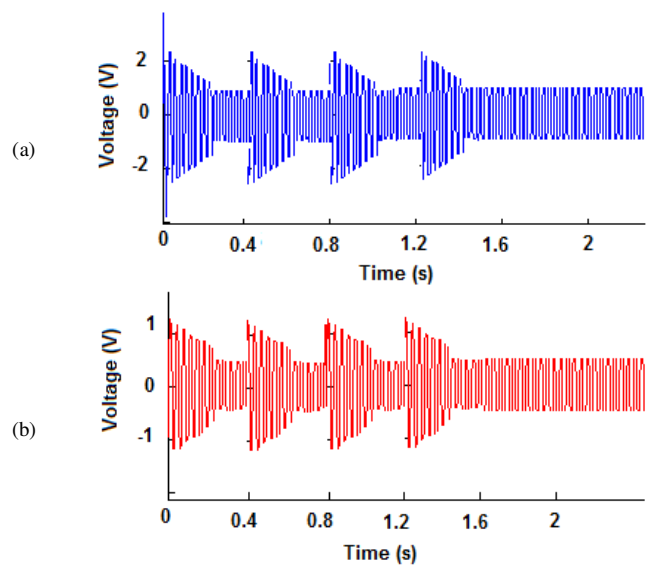

Fig. 14.   Four strain waveforms underwent above the pipe of value (a) 2 V for FBG1 sensor and (b) 1V for FBG2 sensor.

The FBG sensors are stressed by the strain and their wavelength shifts which can be detected by our interrogation system. In addition, the time of the moment strain reaching FBGs can be noted by computing the time delay between the strain waveforms measured by each FBG sensor. Moreover, the STM32 will transfer the wavelength shift into a wave of optical intensity. By using the appropriate parameters of the system, we can have the relationship between the measured voltage and the strain amplitude which stressed the pipe. Figure 14 illustrates the relationships between the output voltage and the amplitude of the strain wave for the two FBG sensors. The difference in the output voltage of the two FBG sensors is caused by the position of the wavelength of each FBG in the reflect spectrum of the interrogation system. In addition, the optical intensity is positive, but, for data processing reasons we also use negative voltage values. From Figure 14, we have used four strain waveforms in 1.6 s. On the other hand, to discover the time delay for the strain wave between FBG1 and FBG2, we used the correlation theory calculation. The obtained results of the correlation have a delay of 188 μs between the strain wave measured by FBG2 and the strain waveform measured by FBG1. Moreover, in this paper we used an FBG sensor with length of 6 mm with sensitivity in the order of 1 pm/με. In addition, the voltage range of STM32 is 5 V with 11-digit

numbers that represent the collected voltage data, hence the precision of the STM 32 voltage data is about $\Delta V = \frac{5}{2048} = 2.441 \cdot 10^{-3}V$. For the PD measured output voltage we have 1 V when we have a shift in the order of 400 pm in the center wavelength of the FBG sensor. Hence, the resolution of the proposed interrogation system is expressed by:

$$\Delta \lambda = 400 \times 10^{-12} \times \frac{\Delta V}{1} = 1 \text{ pm} \qquad (7)$$

The proposed interrogation system gives a sensing resolution about $\Delta \lambda = 1$ pm. So, the minimum strain that can be sensed by this system is 1 µε in the complete C band.

V.   CONCLUSION

In this paper, we propose an interrogation system technique based on midband filter. The proposed system can interrogate the FBG sensors at a speed of 0.4 GHz. The proposed filter overpowers the problem of the difficult adjustment between the active range and the detection measurement. In addition, the proposed system has, in a great percentage, linear response to the wavelength shift. This midband filter is used with correction in the wavelength range of the C band and has been implemented in STM32. The proposed interrogation system of FBG sensors is used to show the monitoring of the strain that stressed a rubber pipe. We used one and then two FBGs and the system can detect well the wavelength shift. The obtained results confirm the low cost of the proposed system, due to the low cost of the used equipment, which has improved sensitivity (1 µε) in comparison with other techniques, that are based on active detection plane.

REFERENCES

[1]   J. Salo and I. Korhonen, "Calculated estimate of FBG sensor's suitability for beam vibration and strain measuring," *Measurement*, vol. 47, pp. 178–183, Jan. 2014, https://doi.org/10.1016/j.measurement.2013.08.017.

[2]   R. Kumar Sah, A. Kumar, A. Gautam, and V. Kumar Rajak, "Temperature independent FBG based displacement sensor for crack detection in civil structures," *Optical Fiber Technology*, vol. 74, Dec. 2022, Art. no. 103137, https://doi.org/10.1016/j.yofte.2022.103137.

[3]   S. Li, Z. Liang, and P. Guo, "A FBG pull-wire vertical displacement sensor for health monitoring of medium-small span bridges," *Measurement*, vol. 211, Apr. 2023, Art. no. 112613, https://doi.org/10.1016/j.measurement.2023.112613.

[4]   S. Saad, "FBG sensors for seismic control and detection in extradosed bridges," *International Journal on Smart Sensing and Intelligent Systems*, vol. 14, no. 1, pp. 1–13, Jan. 2021, https://doi.org/10.21307/ijssis-2021-013.

[5]   M. Mieloszyk, K. Majewska, and W. Ostachowicz, "Application of embedded fibre Bragg grating sensors for structural health monitoring of complex composite structures for marine applications," *Marine Structures*, vol. 76, Mar. 2021, Art. no. 102903, https://doi.org/10.1016/j.marstruc.2020.102903.

[6]   J. Feng and Q. Jiang, "Slip and roughness detection of robotic fingertip based on FBG," *Sensors and Actuators A: Physical*, vol. 287, pp. 143–149, Mar. 2019, https://doi.org/10.1016/j.sna.2019.01.018.

[7]   E. Vorathin, Z. M. Hafizi, A. M. Aizzuddin, M. K. A. Zaini, and K. S. Lim, "Temperature-independent chirped FBG pressure transducer with high sensitivity," *Optics and Lasers in Engineering*, vol. 117, pp. 49–56, Jun. 2019, https://doi.org/10.1016/j.optlaseng.2019.01.012.

[8]   S. Saad and L. Hassine, "Hydrogen detection with FBG sensor technology for disaster prevention," *Photonic Sensors*, vol. 3, no. 3, pp. 214–223, Sep. 2013, https://doi.org/10.1007/s13320-013-0109-4.

[9]   L. Zhang, X. Qiao, W. Bao, Q. Liu, and M. Shao, "Strain and temperature discrimination using a fiber Bragg grating with off-axis inscription," *Optik*, vol. 171, pp. 941–946, Oct. 2018, https://doi.org/10.1016/j.ijleo.2018.06.128.

[10]   X. Zhang, H. Niu, C. Hou, and F. Di, "An edge-filter FBG interrogation approach based on tunable Fabry-Perot filter for strain measurement of planetary gearbox," *Optical Fiber Technology*, vol. 60, Dec. 2020, Art. no. 102379, https://doi.org/10.1016/j.yofte.2020.102379.

[11]   Z. Ding, Z. Tan, X.-X. Su, and D. Cao, "A fast interrogation system of FBG sensors based on low loss jammed-array wideband sawtooth filter," *Optical Fiber Technology*, vol. 48, pp. 128–133, Mar. 2019, https://doi.org/10.1016/j.yofte.2019.01.004.

[12]   S. Deepa and B. Das, "Interrogation techniques for π-phase-shifted fiber Bragg grating sensor: A review," *Sensors and Actuators A: Physical*, vol. 315, Nov. 2020, Art. no. 112215, https://doi.org/10.1016/j.sna.2020.112215.

[13]   Y. Li *et al.*, "A highly precise FBG sensor interrogation system with wavemeter calibration," *Optical Fiber Technology*, vol. 48, pp. 207–212, Mar. 2019, https://doi.org/10.1016/j.yofte.2019.01.006.

[14]   K. Dey, S. Roy, P. Kishore, M. S. Shankar, R. K. Buddu, and R. Ranjan, "Analysis and performance of edge filtering interrogation scheme for FBG sensor using SMS fiber and OTDR," *Results in Optics*, vol. 2, Jan. 2021, Art. no. 100039, https://doi.org/10.1016/j.rio.2020.100039.

[15]   Y. Miao, B. Liu, K. Zhang, and Q. Zhao, "Linear edge and temperature characteristic of tilted fiber Bragg gratings cladding-mode envelope," *Optical Fiber Technology*, vol. 17, no. 4, pp. 286–290, Jul. 2011, https://doi.org/10.1016/j.yofte.2011.05.001.

[16]   L. Fazzi and R. M. Groves, "Demodulation of a tilted fibre Bragg grating transmission signal using α-shape modified Delaunay triangulation," *Measurement*, vol. 166, Dec. 2020, Art. no. 108197, https://doi.org/10.1016/j.measurement.2020.108197.

[17]   L. Carosso, D. Gaiki, S. Bertoldo, and M. Allegretti, "A New Modular Control Board for Pulse-Jet Cleaning of Dust Collector Filter Bags," *Engineering, Technology & Applied Science Research*, vol. 8, no. 2, pp. 2799–2804, Apr. 2018, https://doi.org/10.48084/etasr.1953.

[18]   R. N. John, I. Read, and W. N. MacPherson, "Design considerations for a fibre Bragg grating interrogation system utilizing an arrayed waveguide grating for dynamic strain measurement," *Measurement Science and Technology*, vol. 24, no. 7, Mar. 2013, Art. no. 075203, https://doi.org/10.1088/0957-0233/24/7/075203.

[19]   J. Park, Y. S. Kwon, M. O. Ko, and M. Y. Jeon, "Dynamic fiber Bragg grating strain sensor interrogation with real-time measurement," *Optical Fiber Technology*, vol. 38, pp. 147–153, Nov. 2017, https://doi.org/10.1016/j.yofte.2017.09.011.

[20]   M. Seifouri, M. M. Karkhanehchi, and S. Rohani, "Design of Multi-Layer Optical Fibers with Ring Refractive Index to Reduce Dispersion and Increase Bandwidth in Broadband Optical Networks," *Engineering, Technology & Applied Science Research*, vol. 2, no. 3, pp. 216–220, Jun. 2012, https://doi.org/10.48084/etasr.166.

[21]   S. Bandyopadhyay *et al.*, "Highly efficient free-space fiber coupler with 45° tilted fiber grating to access remotely placed optical fiber sensors," *Optics Express*, vol. 28, no. 11, pp. 16569–16578, May 2020, https://doi.org/10.1364/OE.392170.

[22]   M. A. A. Humayun, M. A. Rashid, A. Kuwana, and H. Kobayashi, "Improvement of Absorption and Emission Phenomena of 1.55µm Quantum Dot Laser using Indium Nitride," *Engineering, Technology & Applied Science Research*, vol. 13, no. 1, pp. 10134–10139, Feb. 2023, https://doi.org/10.48084/etasr.5512.

[23]   I. Floris, J. Madrigal, S. Sales, J. M. Adam, and P. A. Calderón, "Experimental study of the influence of FBG length on optical shape sensor performance," *Optics and Lasers in Engineering*, vol. 126, Mar. 2020, Art. no. 105878, https://doi.org/10.1016/j.optlaseng.2019.105878.

[24]   L. Leffers, B. Roth, and L. Overmeyer, "Evaluation of polymer-based eccentric FBG bending sensor for humidity, strain, temperature and torsion," *Optics and Lasers in Engineering*, vol. 166, Jul. 2023, Art. no. 107568, https://doi.org/10.1016/j.optlaseng.2023.107568.